

# The influence of spontaneously generated coherence and phase of laser fields on optical bistability in a three-level atomic medium: an analytical approach

DOAI LE VAN<sup>1</sup>, PHUONG LE THI MINH<sup>2</sup>, DUNG NGUYEN TIEN<sup>1</sup>,  
KHOA DINH XUAN<sup>1</sup>, BANG NGUYEN HUY<sup>1\*</sup>

<sup>1</sup>Vinh University, 182 Le Duan Street, Vinh City, Vietnam

<sup>2</sup>Sai Gon University, 273 An Duong Vuong Street, Ho Chi Minh City, Vietnam

\*Corresponding author: bangnh@vinhuni.edu.vn

The influence of spontaneously generated coherence and relative phase of laser fields on optical bistability in a three-level atomic medium under electromagnetically induced transparency was studied by using a density matrix theory. An input-output intensity relation of a probe laser field is derived as an analytical function of parameters of a controlling light field, the relative phase, and the spontaneously generated coherence. This function can be fitted with experimental values to be a semi-empirical model which is helpful for finding related applications. It is shown that thresholds and width of the optical bistability hysteresis loop can be manipulated with the controllable parameters. On the other hand, the influence of population relaxation between two ground hyperfine levels on the optical bistability behavior is significant for small coupling field intensity.

Keywords: optical bistability, electromagnetically induced transparency, spontaneously generated coherence.

## 1. Introduction

The optical bistability (OB) is one of the most interesting topics in nonlinear optics because of its potential applications in both optical sciences and photonic technology, as all-optical switching, all-optical memories, optical transistors, and all-optical logic gates and processors. In the early years of OB research concerning resonant atomic media, a great interest was focused on a two-level system [1–3]. Although the usual OB behaviors of the two-level atomic system were observed experimentally, there is still no applications due to only one optical field being employed for both applying and switching fields, thus the lack of control for switching intensity thresholds.

The advent of electromagnetically induced transparency (EIT) [4] was provided by media with interesting properties which have promoted an impressive progress in OB research. Owing to controllable optical properties and giant Kerr nonlinearity [5, 6], both the switching intensity thresholds and the width of the OB loop can be controlled and reduced significantly [7–11]. It has been shown that the OB behaviors can be controlled by either the intensity or the frequency of applied fields. Several reviews on the OB research concerning the EIT media give a deeper insight into the topic and provide lists of original references [12].

Among various sources that generate quantum interferences, there is a mechanism arising from the spontaneous emission processes in atomic/molecular systems with nonorthogonality of electric dipole moments induced by coherent fields. Such interference creates an additional atomic coherence which is called as spontaneously generated coherence (SGC) [13], resulting in the modification of the medium response. In these regards, the effects of SGC on the optical steady-state behaviors in atomic systems were investigated for lasing without inversion (LWI) [14], absorption and dispersion [15], slow light [16], enhancement of Kerr nonlinearity [17] and pulse propagation [18]. It has been shown that the atomic responses under SGC are sensitive to the relative phase of the applied fields [18, 19].

So far, the influence of SGC on the OB in the three-level  $\Lambda$ -type [20–22], cascade-type [23], and  $V$ -type [24, 25] atomic systems was investigated numerically. Numerical methods are powerful for studying dynamic processes. However, finding analytical models for representation of the EIT spectrum [26–28] and related applications (*e.g.*, EIT enhanced Kerr nonlinearity [29, 30], OB [31], controlling group velocity [32]) is of special interest due to its' usefulness. Among the analytical works, nevertheless, there is still lack of analytical representation of OB under the presence of SGC and the relative phase of the interacting light fields. In order to fill this gap, in this work, we develop the analytical model for OB in a three-level  $\Lambda$ -type atomic medium under the presence of the SGC and the relative phase of the interacting fields by using a semi-classical theory and density matrix formalism. Using the model, the influence of the SGC and the relative phase on characteristics of the OB is investigated.

## 2. Theoretical model

We consider a medium of length  $L$  containing  $N$  three-level atoms placed in a unidirectional ring cavity as shown in Fig. 1, which is the same as in [20]. For a simplicity, we assume that both M3 and M4 mirrors are perfectly reflective, whereas both M1 and M2 mirrors are the same, and each has a reflectivity  $R$  and transitivity  $T$ , with  $R + T = 1$ . The medium is excited via the three-level lambda scheme as in Fig. 2a. A strong coupling laser with frequency  $\omega_c$  drives the transition  $|2\rangle \leftrightarrow |3\rangle$  and the weak probe laser with frequency  $\omega_p$  drives the transition  $|2\rangle \leftrightarrow |1\rangle$ . The induced transition dipole moments align as in Fig. 2b. In the ring cavity, a part of the probe field  $E_p$  is circulated in the cavity but not the coupling field  $E_c$ .

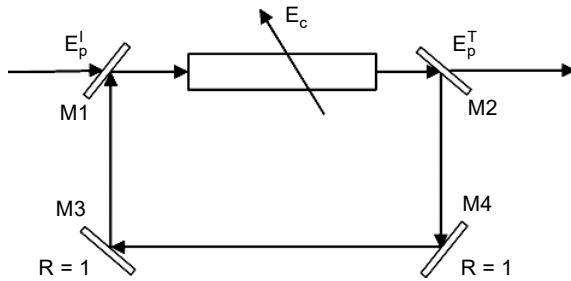


Fig. 1. Schematic setup of a unidirectional ring cavity containing a three-level sample;  $E_p^I$  and  $E_p^T$  denote the incident and transmitted probe field, respectively;  $E_c$  represents the coupling field that is not circulated inside the cavity. Both the coupling and probe beams co-propagate almost collinearly along the atomic cell.

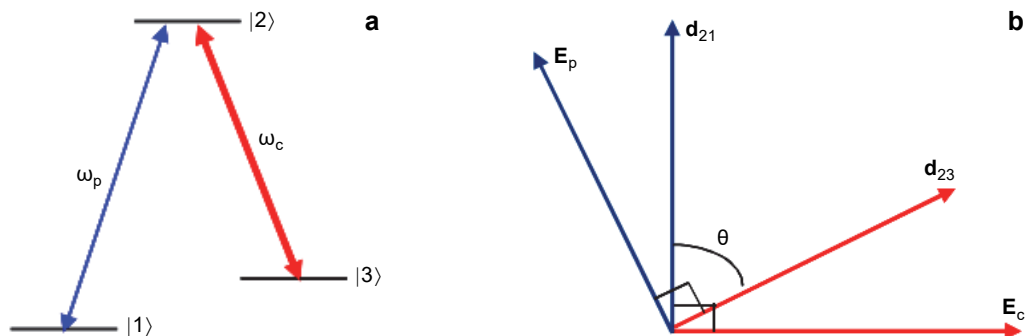


Fig. 2. Three-level lambda excitation scheme (a), and the transition dipole moments induced by the coupling and probe laser fields (b).

Under the slowly varying envelop approximation, the dynamical response of the medium for the probe field is governed by the following wave propagation equation [20]:

$$\frac{\partial E_p}{\partial t} + c \frac{\partial E_p}{\partial z} = i \frac{\omega_p}{2\epsilon_0} P(\omega_p) \quad (1)$$

where,  $c$  and  $\epsilon_0$  are the speed of light and permittivity of free space, respectively,  $P(\omega_p)$  is the induced polarization of the transition  $|2\rangle \leftrightarrow |1\rangle$  given by

$$P(\omega_p) = N d_{21} \rho_{21} \quad (2)$$

where  $d_{21}$  denotes the electric dipole moment, and  $\rho_{21}$  is the corresponding density matrix element.

Under the steady-state regime, the time derivative in Eq. (1) is set to zero, thus, by substituting Eq. (2) into Eq. (1), we obtain the following relation:

$$\frac{\partial E_p}{\partial z} = i \frac{N \omega_p d_{21}}{2c\epsilon_0} \rho_{21} \quad (3)$$

For a single circulation of the probe field in the cavity, we denote the probe field at the beginning and at the end of the sample as  $E_p(0)$  and  $E_p(L)$ , respectively (see Fig. 1). For a perfectly tuned cavity, the boundary conditions in the steady state for the incident and transmitted probe fields are given by [20]:

$$E_p(L) = E_p^T / \sqrt{T} \quad (4)$$

$$E_p(0) = \sqrt{T} E_p^I + R E_p(L) \quad (5)$$

The second term in the right-hand side of Eq. (5) describes the feedback from the mirror, which is an essential requirement for generating OB. By normalizing the incident and transmitted probe fields as:

$$Y = \frac{d_{21} E_p^I}{\hbar \sqrt{T}} \quad (6a)$$

$$X = \frac{d_{21} E_p^T}{\hbar \sqrt{T}} \quad (6b)$$

we obtain the following OB equation for the probe field:

$$Y = X - iC\rho_{21} \quad (7)$$

where

$$C = \frac{N\omega_p L d_{21}^2}{2c\varepsilon_0 \hbar T} \quad (8)$$

is the cooperation parameter of the atomic medium placed in the ring cavity.

Under the dipole and rotating wave approximations, the dynamics of the system is represented by the following density matrix equations:

$$\dot{\rho}_{11} = \Gamma_{31}\rho_{33} - \Gamma_{31}\rho_{11} + \Gamma_{21}\rho_{22} + \frac{i}{2}\Omega_p(\rho_{21} - \rho_{12}) \quad (9)$$

$$\dot{\rho}_{22} = -(\Gamma_{23} + \Gamma_{21})\rho_{22} + \frac{i}{2}\Omega_p(\rho_{12} - \rho_{21}) + \frac{i}{2}\Omega_c(\rho_{32} - \rho_{23}) \quad (10)$$

$$\dot{\rho}_{33} = \Gamma_{31}\rho_{11} - \Gamma_{31}\rho_{33} + \Gamma_{23}\rho_{22} - \frac{i}{2}\Omega_c(\rho_{32} - \rho_{23}) \quad (11)$$

$$\dot{\rho}_{21} = \bar{\gamma}_{21}\rho_{11} + \frac{i}{2}\Omega_p(\rho_{11} - \rho_{22}) + \frac{i}{2}\Omega_c\rho_{31} \quad (12)$$

$$\dot{\rho}_{23} = \bar{\gamma}_{23}\rho_{23} + \frac{i}{2}\Omega_c(\rho_{33} - \rho_{22}) + \frac{i}{2}\Omega_p\rho_{13} \quad (13)$$

$$\dot{\rho}_{31} = \bar{\gamma}_{31}\rho_{31} - \frac{i}{2}\Omega_p\rho_{32} + \frac{i}{2}\Omega_c\rho_{21} + p \exp(i\Phi) \sqrt{\Gamma_{21}\Gamma_{23}} \rho_{22} \quad (14)$$

where  $\Omega_1 = \mathbf{d}_{21} \cdot \mathbf{E}_p / \hbar$  and  $\Omega_2 = \mathbf{d}_{23} \cdot \mathbf{E}_c / \hbar$  are Rabi frequencies induced by the laser fields. We set  $\Omega_1 = \Omega_p \exp(i\Phi_p)$  and  $\Omega_2 = \Omega_c \exp(i\Phi_c)$  with  $\Omega_p$  and  $\Omega_c$  being real parameters;  $\Phi_p$  and  $\Phi_c$  represent phase of the probe and coupling fields, respectively;  $\Gamma_{21}$  and  $\Gamma_{32}$  are the decay rate from the state  $|2\rangle$  to state  $|1\rangle$  and from the state  $|2\rangle$  to state  $|3\rangle$ , respectively;  $\Gamma_{31}$  represents the rate of population relaxation between two hyperfine levels of the ground state,  $|1\rangle$  and  $|3\rangle$ ;  $\bar{\gamma}_{21} = i\Delta_p - \gamma_{21}$ ,  $\bar{\gamma}_{23} = i\Delta_c - \gamma_{23}$  and  $\bar{\gamma}_{31} = i(\Delta_p - \Delta_c) - \gamma_{31}$ ;  $\Delta_p = \omega_p - \omega_{21}$  and  $\Delta_c = \omega_c - \omega_{23}$  are frequency detunings of the coupling and probe laser fields, respectively;  $\gamma_{kl}$  is represented with the decay rates  $\Gamma_{kl}$  from state  $|k\rangle$  to  $|l\rangle$  by the following formula:

$$\gamma_{kl} = \frac{1}{2} \left( \sum_{E_j < E_k} \Gamma_{kj} + \sum_{E_m < E_l} \Gamma_{lm} \right) \quad (15)$$

It should be noted that the term  $p \exp(i\Phi) \sqrt{\Gamma_{21}\Gamma_{23}} \rho_{22}$  represents the SGC resulting from the cross coupling between the spontaneous emissions of the transitions  $|2\rangle \leftrightarrow |1\rangle$  and  $|2\rangle \leftrightarrow |3\rangle$ ;  $p = \mathbf{d}_{21} \cdot \mathbf{d}_{23} / |\mathbf{d}_{21}| |\mathbf{d}_{23}| = \cos\theta$  with  $\theta$  being the angle between the two dipole moments,  $\Phi = \Phi_p - \Phi_c$  is the relative phase between the probe and the coupling fields.

Under the steady regime, after several calculations for Eqs. (9)–(14), we derived the coherence term  $\rho_{21}$  as

$$\begin{aligned} \rho_{21} = & i(\Omega_c A f_1 + \Omega_p f_2) \\ & \times \left\{ \left[ 2\bar{\gamma}_{21}^*(A_{123}^* A_{123} - A_{31} A_{31}^*) - \Omega_c (A_{21} A_{123}^* + A_{31} A_{21}^* - A_{23} A_{123}^*) \right] f_3 \right. \\ & \left. - \Omega_c (A_{31} A_{23}^* - A_{21} A_{123}^* - A_{31} A_{21}^*) \right\}^{-1} \end{aligned} \quad (16)$$

where  $A_{ijk}^*$  and  $\bar{\gamma}_{ij}^*$  are the complex conjugates of  $A_{ijk}$  and  $\bar{\gamma}_{ij}$ , respectively, and

$$\begin{aligned} f_1 = & (A_{31}^* + A_{123}) \frac{2\bar{\gamma}_{21}^*(A_{123}^* A_{123} - A_{31} A_{31}^*) - \Omega_c (A_{21} A_{123}^* + A_{31} A_{21}^* - A_{23} A_{123}^*)}{\Omega_c (A_{31}^* A_{23} - A_{31}^* A_{123} - A_{31}^* A_{21})} \\ & - (A_{31} + A_{123}) \end{aligned} \quad (17)$$

$$\begin{aligned} f_2 = & (A_{123}^* A_{123} - A_{31} A_{31}^*) - \left[ (A_{123} A_{123}^* - A_{31} A_{31}^*) \right. \\ & \times \left. \frac{2\bar{\gamma}_{21}^*(A_{123}^* A_{123} - A_{31} A_{31}^*) - \Omega_c (A_{21} A_{123}^* + A_{31} A_{21}^* - A_{23} A_{123}^*)}{\Omega_c (A_{31}^* A_{23} - A_{21}^* A_{123} - A_{31}^* A_{21})} \right] \end{aligned} \quad (18)$$

$$f_3 = \frac{2\bar{\gamma}_{21}(A_{123}A_{123}^* - A_{31}A_{31}^*) - \Omega_c(A_{21}^*A_{123} + A_{31}^*A_{21} - A_{23}^*A_{123})}{\Omega_c(A_{31}^*A_{23} - A_{21}^*A_{123} - A_{31}^*A_{21})} \quad (19)$$

$$A_0 = \frac{p \exp(i\varphi) \sqrt{\Gamma_{21}\Gamma_{23}}}{\Gamma_{23} + \Gamma_{21}} \quad (20)$$

$$A_1 = \Omega_c \left\{ (\Omega_p^2 - \Omega_c^2)(\Gamma_{23} - 3\Gamma_{31}) - \Omega_c(\Gamma_{23} + \Gamma_{21}) [\Omega_p(A_0 + A_0^*) - \Omega_c] \right\} \quad (21)$$

$$A = 2\Omega_c\Omega_p\Gamma_{31}(\Gamma_{23} + \Gamma_{21}) [\Omega_p - \Omega_c(A_0 + A_0^*)] \quad (22)$$

$$\begin{aligned} A_{123} = & 16\bar{\gamma}_{31}^*\bar{\gamma}_{23}\Gamma_{31}(\Gamma_{23} + \Gamma_{21}) [\Omega_p - \Omega_c(A_0 + A_0^*)] \\ & + 4\Omega_p^2\Gamma_{31}(\Gamma_{23} + \Gamma_{21}) [\Omega_p - \Omega_c(A_0 + A_0^*)] \\ & + \bar{\gamma}_{31}^* [16\Gamma_{31}(\Gamma_{23} + \Gamma_{21})\bar{\gamma}_{23}A_0^*\Omega_c - 2\Omega_p\Omega_c^*(\Gamma_{23} + 3\Gamma_{31})] \end{aligned} \quad (23)$$

$$A_{23} = 8\bar{\gamma}_{23}\Omega_c\Gamma_{31}(\Gamma_{23} + \Gamma_{21}) [\Omega_p - \Omega_c(A_0 + A_0^*)] \quad (24)$$

$$A_{21} = A_1\Omega_p + A_0^*\bar{\gamma}_{23}(\Omega_p^2 - \Omega_c^2)8\Gamma_{31}(\Gamma_{23} + \Gamma_{21}) \quad (25)$$

$$A_{31} = -\bar{\gamma}_{31} [16\Gamma_{31}(\Gamma_{23} + \Gamma_{21})\bar{\gamma}_{23}A_0^*\Omega_c - 2\Omega_p\Omega_c^2(\Gamma_{21} + 3\Gamma_{31})] \quad (26)$$

### 3. Analysis of OB properties

In principle, the OB equation (7) in which the matrix element  $\rho_{21}$  determined by Eq. (16) can be employed to any atomic or molecular systems, has spectroscopic structure as in Fig. 2. As an illustration, we have applied it to the case of cold atomic medium of  $^{87}\text{Rb}$ , where Doppler effect can be ignored. In this case, the states  $|1\rangle$ ,  $|2\rangle$ , and  $|3\rangle$  are chosen as  $5S_{1/2}(F=1)$ ,  $5P_{3/2}(F'=2)$  and  $5S_{1/2}(F''=2)$ , respectively; the decay rates given by [33] are:  $\Gamma_{21} = \Gamma_{23} = 6\gamma = 6$  MHz, and  $\Gamma_{31} = 0.003\gamma$ .

First of all, we considered the influence of SGC by making a surface plot of the input-output fields vs. the interference parameter  $p$  when keeping the relative phase at  $\Phi = 0$ , as in Fig. 3a. Also, OB curves determined at specific values of the parameter  $p$  are plotted in Fig. 3b. It is clear that both OB width and switching thresholds increase with a growing value of the parameter  $p$ . To explain this propensity, we plotted the absorption vs.  $p$  as in Fig. 4. It shows that the absorption is grown as the SGC increases, which leads to increasing the needed value to attain the particular switching thresholds.

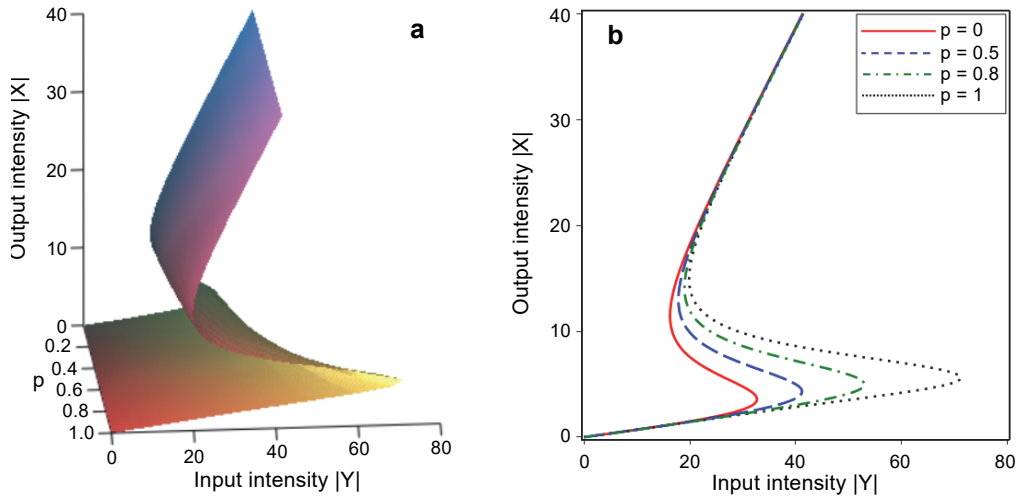


Fig. 3. Surface plots of input-output intensity relation *vs.* the parameter  $p$  when  $\Phi = 0$ ,  $\Omega_c = 4\gamma$ ,  $A_c = 0$ ,  $A_p = 4\gamma$ , and  $C = 80\gamma$  **(a)**; OB curves at specific values of the parameters  $p$  **(b)**.

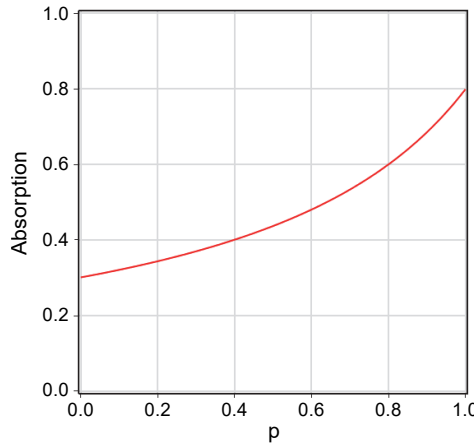


Fig. 4. Variation of the absorption (imaginary part of  $\rho_{21}$ ) *vs.* the parameter  $p$ , where the remaining parameters are given the same as in Fig. 3.

Next, we studied the influence of the relative phase  $\Phi$  by plotting the OB surface and OB curves at specific values of  $\Phi$ , as shown in Fig. 5. The switching thresholds and width of OB depend periodically on the relative phase with a period  $2\pi$ . This behavior can be explained by noting the variation of the probe absorption ( $\text{Im}\rho_{21}$ ) *vs.* the relative phase, as in Fig. 6. It can be seen that the absorption is also changed periodically with the same period. As indicated in [2], such a change of absorption is a reason for the periodical change of the OB width and thresholds. Indeed, Figs. 5a and 6 show

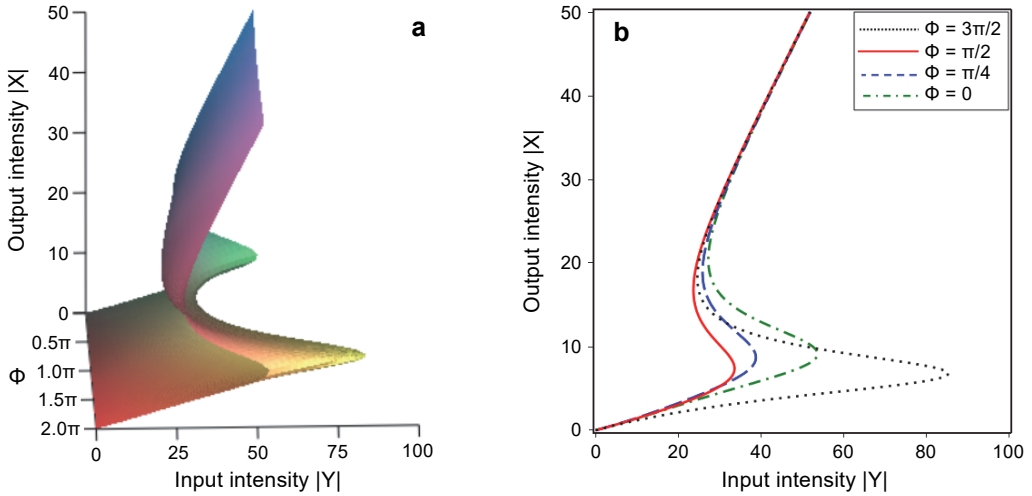


Fig. 5. Surface plots of OB vs. the relative phase  $\Phi$  when  $p = 0.9$ ,  $\Omega_c = 4\gamma$ ,  $\Delta_c = 0$ ,  $\Delta_p = 4\gamma$ , and  $C = 80\gamma$  (**a**); OB curves at specific values of the relative phase (**b**).

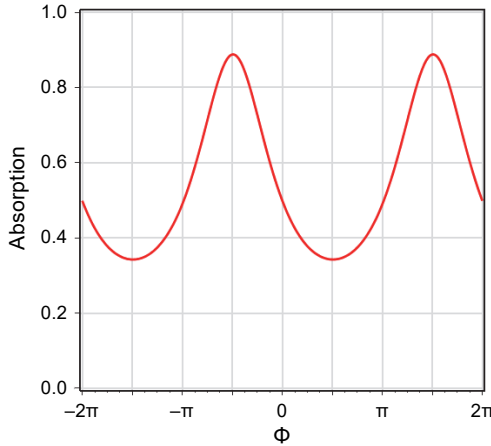


Fig. 6. Variation of the absorption vs. the relative phase  $\Phi$ , the remaining parameters are given the same as in Fig. 5.

that the biggest absorption (attains at  $\Phi = 3\pi/2$ ) or smallest absorption (attains at  $\Phi = \pi$ ) correspond to the largest OB or smallest OB width, respectively.

The variations of the input-output fields vs. the probe frequency detuning (with the fixed values  $\Omega_c = 4\gamma$ ,  $\Delta_c = 0$ ,  $p = 0.9$ ,  $\Phi = 0$ , and  $C = 80\gamma$ ) are shown in Fig. 7a. The OB curves at specific values of  $\Delta_p$  are also plotted in Fig. 7b. There is no OB behavior when  $\Delta_p = 0$  because of the zero nonlinearity (see [29]). However, both the OB width and switching thresholds increase when  $\Delta_p$  varies from 0 to  $-2\gamma$ , and they are decreased when  $\Delta_p$  varies from  $-2\gamma$  to  $-10\gamma$ .

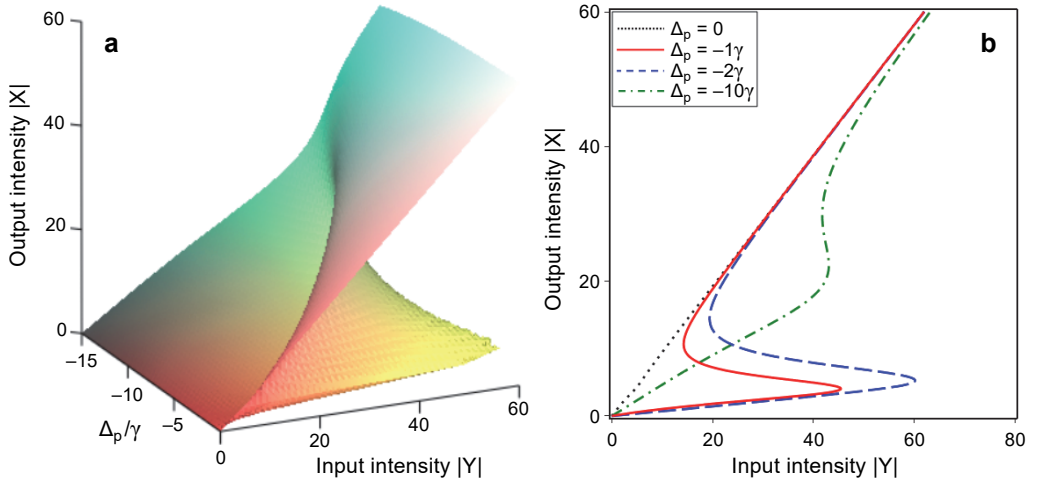


Fig. 7. Surface plots of the OB vs. the probe detuning (in negative region) at  $p = 0.9$ ,  $\Phi = 0$ ,  $\Omega_c = 4\gamma$ ,  $A_c = 0$ , and  $C = 80\gamma$  (a). OB curves at specific values of the probe detuning, other parameters are similar to those in a (b).

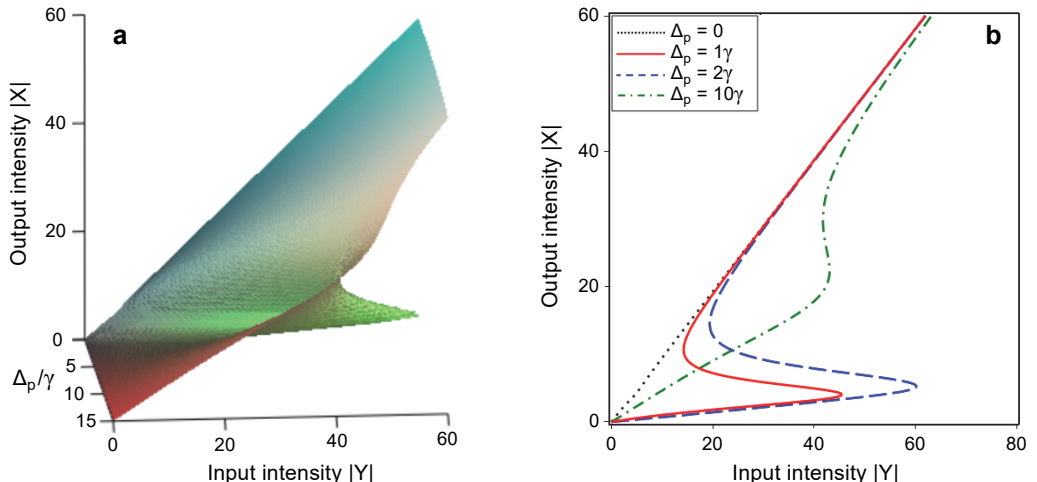


Fig. 8. Surface plots of OB when  $p = 0.9$ ,  $\Phi = 0$ ,  $\Omega_c = 4\gamma$ ,  $A_c = 0$ , and  $C = 80\gamma$  (a). OB curves at specific values of the probe detuning, other parameters are similar to those in the case a (b).

Due to the symmetry of the nonlinear curve over the point  $\Delta_p = 0$  (see [29]), the OB behaviors in positive detuning are similar to those in negative detuning, as shown in Fig. 8. We also see that both the OB width and thresholds increase when  $\Delta_p$  varies from 0 to  $2\gamma$ , and they decrease as  $\Delta_p$  varies from  $2\gamma$  to  $10\gamma$ .

The influence of intensity and frequency of the coupling laser field on the OB behavior is shown in Figs. 9 and 10, respectively. Here, the values of the probe frequency

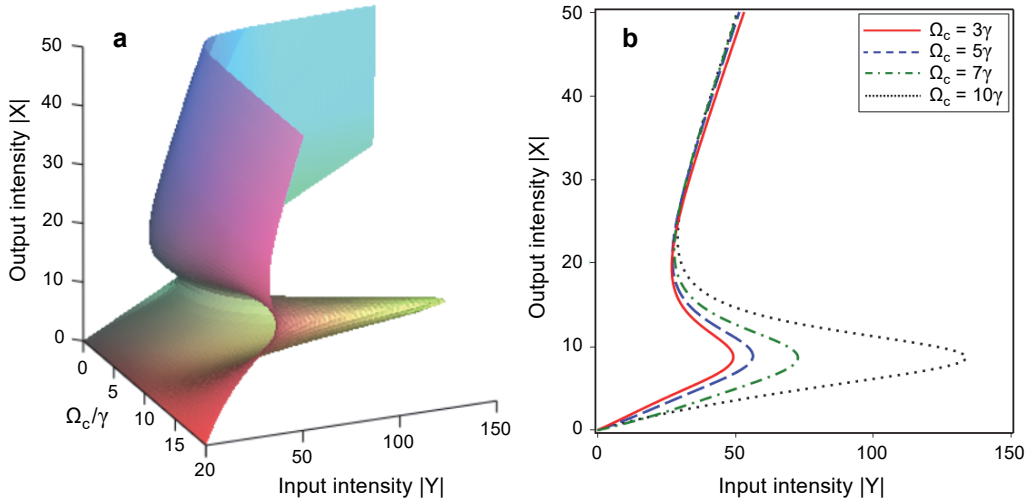


Fig. 9. Surface plot of OB when  $p = 0.9$ ,  $\Phi = 0$ ,  $\Delta_p = 4\gamma$ ,  $\Delta_c = 0$ , and  $C = 80\gamma$  (a); OB curves at specific values of coupling intensity  $\Omega_c$  (b).

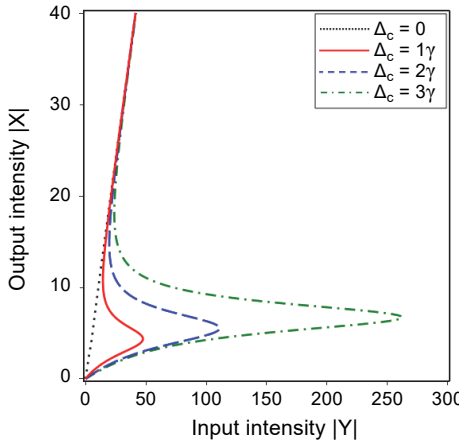


Fig. 10. OB curves determined at specific values of the coupling frequency detuning  $\Delta_c$ , where  $p = 0.9$ ,  $\Phi = 0$ ,  $\Delta_p = 2\gamma$ ,  $\Omega = 4\gamma$ , and  $C = 80\gamma$ .

detuning and the strength of the SGC are chosen as  $\Delta_p = 0$  and  $p = 0.9$ . From these figures one can see the controllable OB thresholds/width by changing the intensity or/and frequency detuning of the coupling field.

The influence of the cooperation parameter  $C$  on OB is plotted in Fig. 11, where the parameters of the probe and coupling lasers are fixed at  $\Delta_p = 4\gamma$ ,  $\Delta_c = 0$ , and  $\Omega_c = 4\gamma$ . It is apparent to see that an increase in the cooperative parameter leads to a broader OB width. Such behavior can be explained by the fact that increasing  $C$  leads to increased absorption ( $C$  is proportional to the atomic density) or increased attenuation, resulting in a higher intensity needed to attain OB thresholds.

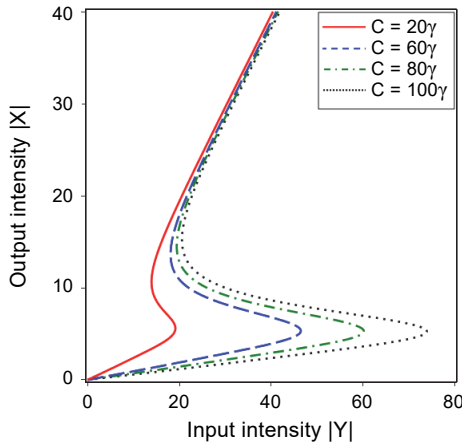


Fig. 11. OB curves determined at specific values of  $C$ , where  $p = 0.9$ ,  $\Phi = 0$ ,  $\Delta_p = 4\gamma$ ,  $\Delta_c = 0$ , and  $\Omega_c = 4\gamma$ .

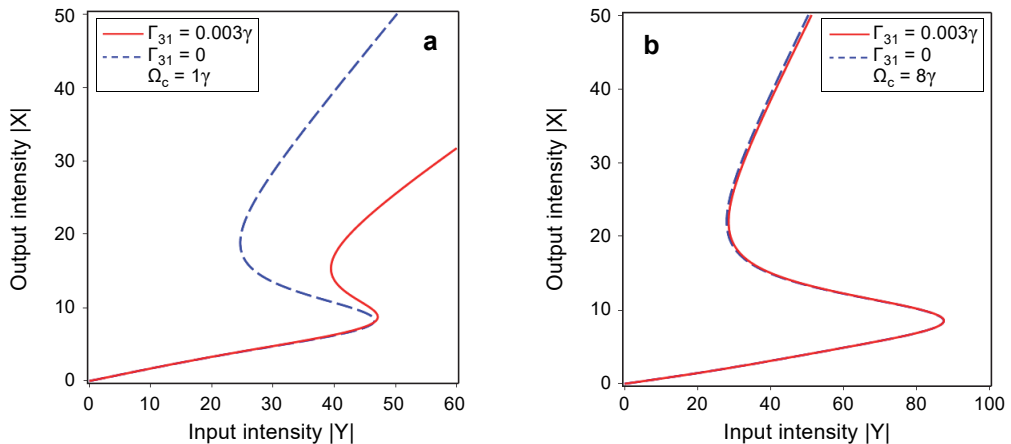


Fig. 12. OB curves determined at  $\Gamma_{31} = 0.003\gamma$  (solid line) and  $\Gamma_{31} = 0$  (dashed line) for different values of the coupling intensity,  $\Omega_c = 1\gamma$  (a) and  $\Omega_c = 8\gamma$  (b). The other parameters are  $\Delta_p = 4\gamma$ ,  $\Delta_c = 0$ ,  $p = 0.9$ ,  $\Phi = 0$ , and  $C = 80\gamma$ .

Finally, we considered the influence of the population relaxation  $\Gamma_{31}$  between two hyperfine states  $|1\rangle$  and  $|3\rangle$  by plotting the OB curves for two cases,  $\Gamma_{31} = 0.003\gamma$  (solid curve) and  $\Gamma_{31} = 0$  (dashed curve), as shown in Fig. 12. The comparison shows a minor deviation for strong coupling laser intensity (Fig. 12b), however, it is significant for small coupling laser intensity (Fig. 12a).

## 4. Conclusions

We have studied the OB in the three-level  $A$ -type atomic medium under the SGC and the relative phase between the probe and coupling laser fields. The OB equation has been derived as an analytical function of controllable parameters of the intensity, frequency

and relative phase of the laser fields, and SGC. It is found that the switching intensity thresholds, thus the OB hysteresis loop, can be manipulated with the controllable parameters. Under SGC, the OB switching thresholds and width can be changed periodically with the relative phase at period  $2\pi$  due to modification of absorption. On the other hand, for the case of small coupling intensity, the influence of population relaxation between two hyperfine levels  $|1\rangle$  and  $|3\rangle$  on the OB curve is significant. This is important for experiments where the population relaxation depends on temperature of the atomic sample. The analytical OB relation may be employed to fit with experimentally observed values to be a semi-empirical model which is helpful for several related applications.

*Acknowledgments* – The financial support from Vietnamese National Foundation of Science and Technology Development (NAFOSTED) through the grant code 103.03-2017.332 is acknowledged.

## References

- [1] ABRAHAM E., SMITH S.D., *Optical bistability and related devices*, Reports on Progress in Physics **45**(8), 1982, pp. 815–885.
- [2] LUGIATO L.A., *II. Theory of optical bistability*, Progress in Optics **21**, 1984, pp. 69–216, DOI: [10.1016/S0079-6638\(08\)70122-7](https://doi.org/10.1016/S0079-6638(08)70122-7).
- [3] GIBBS H.M., *Optical Bistability: Controlling Light with Light*, Academic Press, New York, 1985, DOI: [10.1016/B978-0-12-281940-7.X5001-X](https://doi.org/10.1016/B978-0-12-281940-7.X5001-X).
- [4] BOLLER K.-J., IMAMOGLU A., HARRIS S.E., *Observation of electromagnetically induced transparency*, Physical Review Letters **66**(20), 1991, p. 2593, DOI: [10.1103/PhysRevLett.66.2593](https://doi.org/10.1103/PhysRevLett.66.2593).
- [5] HARRIS S.E., HAU L.V., *Nonlinear optics at low light levels*, Physical Review Letters **82**(23), 1999, p. 4611, DOI: [10.1103/PhysRevLett.82.4611](https://doi.org/10.1103/PhysRevLett.82.4611).
- [6] WANG H., GOORSKEY D., XIAO M., *Enhanced Kerr nonlinearity via atomic coherence in a three-level atomic system*, Physical Review Letters **87**(7), 2001, article ID 073601, DOI: [10.1103/PhysRevLett.87.073601](https://doi.org/10.1103/PhysRevLett.87.073601).
- [7] BERGOU J., ZHAO D., *Effect of a squeezed vacuum input on optical bistability*, Physical Review A **52**(2), 1995, pp. 1550–1560, DOI: [10.1103/PhysRevA.52.1550](https://doi.org/10.1103/PhysRevA.52.1550).
- [8] GONG S., DU S., XU Z., PAN S., *Optical bistability via a phase fluctuation effect of the control field*, Physics Letters A **222**(4), 1996, pp. 237–240, DOI: [10.1016/0375-9601\(96\)00637-8](https://doi.org/10.1016/0375-9601(96)00637-8).
- [9] WANG H., GOORSKEY D.J., XIAO M., *Bistability and instability of three-level atoms inside an optical cavity*, Physical Review A **65**(1), 2002, article ID 011801(R), DOI: [10.1103/PhysRevA.65.011801](https://doi.org/10.1103/PhysRevA.65.011801).
- [10] JOSHI A., XIAO M., *Optical multistability in three-level atoms inside an optical ring cavity*, Physical Review Letters **91**(14), 2003, article ID 143904, DOI: [10.1103/PhysRevLett.91.143904](https://doi.org/10.1103/PhysRevLett.91.143904).
- [11] JOSHI A., BROWN A., WANG H., XIAO M., *Controlling optical bistability in a three-level atomic system*, Physical Review A **67**(4), 2003, article ID 041801(R), DOI: [10.1103/PhysRevA.67.041801](https://doi.org/10.1103/PhysRevA.67.041801).
- [12] JOSHI A., XIAO M., *Controlling Steady-State and Dynamical Properties of Atomic Optical Bistability*, World Scientific Publishing, 2012, DOI: [10.1142/7766](https://doi.org/10.1142/7766).
- [13] JAVANAINEN J., *Effect of state superpositions created by spontaneous emission on laser-driven transitions*, Europhysics Letters **17**(5), 1992, pp. 407–412.
- [14] MA H., GONG S., LIU C., SUN Z., XU Z., *Effects of spontaneous emission-induced coherence on population inversion in a ladder-type atomic system*, Optics Communications **223**(1–3), 2003, pp. 97–101, DOI: [10.1016/S0030-4018\(03\)01572-4](https://doi.org/10.1016/S0030-4018(03)01572-4).

- [15] MA HONG-MEI, GONG SHANG-QING, SUN ZHEN-RONG, LI RU-XIN, XU ZHI-ZHAN, *Effects of spontaneously induced coherence on absorption of a ladder-type atom*, Chinese Physics **15**(11), 2006, pp. 2588–2592, DOI: [10.1088/1009-1963/15/11/022](https://doi.org/10.1088/1009-1963/15/11/022).
- [16] BAI Y., GUO H., HAN D., SUN H., *Effects of spontaneously generated coherence on the group velocity in a V system*, Physics Letters A **340**(1–4), 2005, pp. 342–346, DOI: [10.1016/j.physleta.2005.03.069](https://doi.org/10.1016/j.physleta.2005.03.069).
- [17] NIU Y., GONG S., *Enhancing Kerr nonlinearity via spontaneously generated coherence*, Physical Review A **73**(5), 2006, article ID 053811, DOI: [10.1103/PhysRevA.73.053811](https://doi.org/10.1103/PhysRevA.73.053811).
- [18] DONG HOANG MINH, DOAI LE VAN, BANG NGUYEN HUY, *Pulse propagation in an atomic medium under spontaneously generated coherence, incoherent pumping, and relative laser phase*, Optics Communications **426**, 2018, pp. 553–557, DOI: [10.1016/j.optcom.2018.06.008](https://doi.org/10.1016/j.optcom.2018.06.008).
- [19] LI A., MA H., TAN X., YANG Y., TONG D., FAN X., *Phase control of probe response in an open ladder type system with spontaneously generated coherence*, Optics Communications **280**(2), 2007, pp. 397–403, DOI: [10.1016/j.optcom.2007.08.049](https://doi.org/10.1016/j.optcom.2007.08.049).
- [20] JOSHI A., YANG W., XIAO M., *Effect of spontaneously generated coherence on optical bistability in three-level A-type atomic system*, Physics Letters A **315**(3–4), 2003, pp. 203–207, DOI: [10.1016/S0375-9601\(03\)01046-6](https://doi.org/10.1016/S0375-9601(03)01046-6).
- [21] LIU C., GONG S., FAN X., XU Z., *Phase control of spontaneously generated coherence induced bistability*, Optics Communications **239**(4–6), 2004, pp. 383–388, DOI: [10.1016/j.optcom.2004.06.003](https://doi.org/10.1016/j.optcom.2004.06.003).
- [22] WANG Z., CHEN A.-X., BAI Y., YANG W.-X., LEE R.-K., *Coherent control of optical bistability in an open A-type three-level atomic system*, Journal of the Optical Society of America B **29**(10), 2012, pp. 2891–2896, DOI: [10.1364/JOSAB.29.002891](https://doi.org/10.1364/JOSAB.29.002891).
- [23] CHENG D., LIU C., GONG S., *Optical bistability and multistability via the effect of spontaneously generated coherence in a three-level ladder-type atomic system*, Physics Letters A **332**(3–4), 2004, pp. 244–249, DOI: [10.1016/j.physleta.2004.09.052](https://doi.org/10.1016/j.physleta.2004.09.052).
- [24] JOSHI A., YANG W., XIAO M., *Effect of quantum interference on optical bistability in the three-level V-type atomic system*, Physical Review A **68**(1), 2003, article ID 015806, DOI: [10.1103/PhysRevA.68.015806](https://doi.org/10.1103/PhysRevA.68.015806).
- [25] LI J., *Coherent control of optical bistability in a microwave-driven V-type atomic system*, Physica D: Nonlinear Phenomena **228**(2), 2007, pp. 148–152, DOI: [10.1016/j.physd.2007.03.002](https://doi.org/10.1016/j.physd.2007.03.002).
- [26] DOAI L.V., TRONG P.V., KHOA D.X., BANG N.H., *Electromagnetically induced transparency in five-level cascade scheme of  $^{85}\text{Rb}$  atoms: an analytical approach*, Optik **125**(14), 2014, pp. 3666–3669, DOI: [10.1016/j.ijleo.2014.01.080](https://doi.org/10.1016/j.ijleo.2014.01.080).
- [27] KHOA D.X., TRONG P.V., DOAI L.V., BANG N.H., *Electromagnetically induced transparency in a five-level cascade system under Doppler broadening: an analytical approach*, Physica Scripta **91**(3), 2016, article ID 035401, DOI: [10.1088/0031-8949/91/3/035401](https://doi.org/10.1088/0031-8949/91/3/035401).
- [28] KHOA D.X., TRUNG L.C., THUAN P.V., DOAI L.V., BANG N.H., *Measurement of dispersive profile of a multiwindow electromagnetically induced transparency spectrum in a Doppler-broadened atomic medium*, Journal of the Optical Society of America B **34**(6), 2017, pp. 1255–1263, DOI: [10.1364/JOSAB.34.001255](https://doi.org/10.1364/JOSAB.34.001255).
- [29] KHOA D.X., DOAI L.V., SON D.H., BANG N.H., *Enhancement of self-Kerr nonlinearity via electromagnetically induced transparency in a five-level cascade system: an analytical approach*, Journal of the Optical Society of America B **31**(6), 2014, pp. 1330–1334, DOI: [10.1364/JOSAB.31.001330](https://doi.org/10.1364/JOSAB.31.001330).
- [30] DOAI L.V., KHOA D.X., BANG N.H., *EIT enhanced self-Kerr nonlinearity in the three-level lambda system under Doppler broadening*, Physica Scripta **90**(4), 2015, article ID 045502, DOI: [10.1088/0031-8949/90/4/045502](https://doi.org/10.1088/0031-8949/90/4/045502).
- [31] KHOA D.X., DOAI L.V., ANH L.N.M., TRUNG L.C., THUAN P.V., DUNG N.T., BANG N.H., *Optical bistability in a five-level cascade EIT medium: an analytical approach*, Journal of the Optical Society of America B **33**(4), 2016, pp. 735–740, DOI: [10.1364/JOSAB.33.000735](https://doi.org/10.1364/JOSAB.33.000735).

- [32] ANH N.T., DOAI L.V., BANG N.H., *Manipulating multi-frequency light in a five-level cascade type atomic medium associated with giant self-Kerr nonlinearity*, Journal of the Optical Society of America B **35**(6), 2018, pp. 1233–1239, DOI: [10.1364/JOSAB.35.001233](https://doi.org/10.1364/JOSAB.35.001233).
- [33] STECK D.A.,  $^{87}\text{Rb}$  *D Line Data*, <http://steck.us/alkalidata>

*Received November 4, 2018  
in revised form March 7, 2019*